American Journal of Pathology, Vol. 164, No. 5, May 2004

Expression of Myopodin Induces Suppression of Tumor Growth and Metastasis

Ling Jing,* Lijun Liu,* Yan Ping Yu,* Rajiv Dhir,* Marie Acquafondada,* Doug Landsittel,† Kathleen Cieply,* Alan Wells,* and Jian-Hua Luo*

From the Department of Pathology and the Biostatistic Center,† University of Pittsburgh School of Medicine, Pittsburgh, Pennsylvania*

Myopodin was previously reported as a gene that was frequently deleted in prostate cancer. This gene shares significant homology with a cell shape-regulating gene, synaptopodin. Myopodin was shown to bind actin and to induce actin bundling when cells were stimulated. To clarify the functional role of myopodin in prostate cancer, several assays were performed to evaluate the tumor suppression activity of myopodin. Our results indicate that myopodin inhibits tumor growth and invasion both *in vitro* and *in vivo*. The activity of tumor suppression of myopodin is located at the C-terminus region. To further evaluate the role of myopodin in suppressing the invasiveness of prostate cancer, an expression analysis of myopodin protein was performed in prostate tissues. The results indicate that down-regulation of myopodin expression occurs mostly in invasive stages of prostate cancer, implying a potential invasion suppression role for myopodin in prostate cancer. In addition, hemizygous deletion and down-regulation of myopodin expression occur in three aggressive prostate cancer cell lines. All these results support the hypothesis that myopodin functions as a tumor suppressor gene to limit the growth and to inhibit the metastasis of cancer cells. *(Am J Pathol 2004, 164:1799–1806)*

Prostate cancer is second only to skin cancer as the most commonly diagnosed malignancies in American men: at current rates of diagnosis, one man in six will be diagnosed with the disease during his lifetime.[1] Approximately 30,000 men die from this disease annually.[1] Epidemiological and laboratory studies indicate that genetic changes contribute to the pathogenesis of prostate cancers.[2] Nineteen of the 23 pairs of chromosomes are implicated in subsets of prostate cancers.[2] The aberrant genomic alterations seem to accumulate with advancing stages of prostate cancers. Against this backdrop of a very common malignancy, it is still not clear what key molecular events are responsible for the progression of initial prostate cancer development to the lethal form of the disease.

Myopodin was initially identified as a gene frequently deleted in advanced stage prostate cancer.[3] Another study indicated that myopodin regulated myocyte differentiation and was involved in stress-induced formation of actin bundling.[4] However, as myopodin is present also in nonmuscle cells, much of the function of myopodin remains unexplored. Myopodin contains in its C-terminus region a significant homology with synaptopodin, a protein regulating synaptic spine formation and mediating cell-cell contact.[5,6] Despite scanty information of myopodin, some of its functions may be related to its homology with its closest known relative, synaptopodin. Synaptopodin was originally identified as an actin-binding protein exclusively expressed in kidney podocytes and neurons.[5] It modulates cytoskeleton rearrangement during foot process formation.[6] It is also involved in changing the shape of synaptic spine and maintaining synaptic contact of neurons.[7] Mice with homozygous deletion of synaptopodin demonstrate defects of spine apparatus and learning deficiency.[8]

In this study, we investigated the potential tumor suppression function of myopodin using both an androgen-dependent and -independent human prostate tumor cell line, both *in vitro* and in animal models. These experiments consistently indicated that myopodin contained tumor growth and invasion suppression activities. The tumor suppression activity of myopodin is located at the C-terminus region. In addition, a survey study of myopodin expression in prostate cancer samples suggests an inverse relationship between prostate cancer progression and expression of the myopodin protein.

Materials and Methods

Materials

PC3, DU145, and LNCaP cell lines were purchased from American Type Culture Collection, Inc. (Manassas, VA). The Matrigel transmigration kit was purchased from Becton Dickinson Labware (Bedford, MA). Severe combined

Supported by the United States Department of Defense (grant DAMD17 03 1 0147) and the National Cancer Institute (grant 1UO1CA88110-01).

L.J. and L.L. contributed equally to this article.

Accepted for publication January 29, 2004.

Address reprint requests to Jian-Hua Luo, Scaife Hall A-725, 3550 Terrace St., Pittsburgh, PA 15261. E-mail: luoj@msx.upmc.edu.

immunodeficiency disease (SCID) mice were purchased from Taconic, Inc. (New York, NY). Myopodin antisera were raised through immunized rabbits with peptides corresponding to regions of myopodin coding sequences (CQTDGLRTTTSYQRKEEES-myoN, FKGPQAAVASQNYTPKPTVS-myoB, KMGKKKGKKPLNALDVMKHQ-myoC).

Generation of Antibodies against Myopodin

Three antisera were raised from rabbits against regions of myopodin nonhomologous to synaptopodin, covering amino terminus (myoN), middle third (myoB), and C-terminus (myoC). These antisera were peptide affinity-purified using the aminolink kit from Pierce (Rockford, IL). The purified antisera were tested for specificity for myopodin in Western blot with protein extracts from cells known to overexpress myopodin (I4) or cells not expressing myopodin (LNCaP, 293 cells). All three antisera detected a single band of 83-kd protein (the predicted molecular weight of myopodin) in I4 or PC3 cells but were negative in LNCaP and 293 cells. The antisera were then titrated for antibody avidity. All three antisera detected the single myopodin band at the titration of at least a 1:5000 dilution. Synaptopodin is the only protein containing significant homology to myopodin, but has a significantly higher molecular weight (110 kd). Also, the myopodin antisera were raised to sequences containing no homology to synaptopodin. Therefore, it is extremely unlikely that the only 83-kd band detected by three different antisera represents a cross reaction with synaptopodin.

Construction of Stable Myopodin and Its Deletion Mutants Expressing PC-3 and LNCaP Cells

The 4.4-kb mRNA of myopodin encodes a 698-amino acid protein. The full-length cDNA was amplified using primers E1/E4 (GCATTGCCCTTCTTCTAACGGA/ATAGCAGATTGACAGTGACAGC) on templates obtained from a cDNA library of normal prostate gland, using extended polymerase chain reaction (PCR) protocols (Hoffman-La Roche, Nutley, NJ). The PCR products were ligated into TOPO TA cloning vector pCR2.1. The construct was subsequently digested with *Bam*HI and *Apa*I, and ligated into the similarly restricted pCMV-Script vector. The pCMV-myopodin construct was sequenced and confirmed that no mutation was introduced into the insert during the cloning process. Deletion mutants of myopodin were constructed by digesting the pCMV-myopodin construct with *Apa*I and *Pst*I, and *Apa*I and *Xho*I, and generating 5.0- and 5.8-kb fragments, respectively. These constructs represent deletions of C-terminus of myopodin by 470 (5.0) and 197 (5.9) amino acids at the C-terminus, respectively. The constructs were transfected into PC-3 and LNCaP cells using the protocols of Superfect (Valencia, CA). Stable myopodin expression cell lines were generated through G418 selection.

Immunoblot Detection of Myopodin

To examine the myopodin expression, the cells were washed with phosphate-buffered saline (PBS) and lysed by RIPA buffer (50 mmol/L Tris-HCl, pH 7.4; 1% Nonidet P-40; 0.25% Na-deoxycholate; 150 mmol/L NaCl; 1 mmol/L ethylenediaminetetraacetic acid; 1 mmol/L phenylmethyl sulfonyl fluoride; 1 μg/ml each of aprotinin, leupeptin, pepstatin; 1 mmol/L Na_3VO_4). The lysates were sonicated and centrifuged to remove the insoluble materials. The proteins were resolved in sodium dodecyl sulfate-polyacrylamide gel electrophoresis in 8.5% polyacrylamide gel, and blotted onto a polyvinylidene difluoride membrane. The membrane was blocked with 5% powdered skim milk in Tris-Tween 20 buffer, pH 7.4, for 1 hour in room temperature, followed by 2 hours of incubation of primary anti-myopodin antibodies. The membrane was then washed three times with Tris-Tween 20 buffer and incubated with horseradish peroxidase-conjugated secondary antibody for 1 hour at room temperature. The myopodin expression was detected with the enhanced chemiluminescence system (Amersham Life Science, Piscataway, NJ) according to the manufacturer's protocols.

Cell Proliferation Assay and Colony Formation Assay

Eight thousand cells were plated triplicate on 35-mm dishes. Cell numbers were quantified at the indicated period of time with 0.4% trypan blue staining. For colony formation assay, 5000 cells were plated in 60-mm dishes. Triplicate experiments were performed for each cell clones. Medium was changed every 4 days. On the10th day, the plates were stained with 1% crystal violet and colonies were quantified.

Soft Agar Colony Formation Assay

Five thousand cells were plated and grown on a plate containing 2% base agar and 0.43% top agar. Cells were incubated at 37°C for 21 days. Plates were stained with 0.005% crystal violet for 1 hour. Colonies were counted under a dissecting microscope.

Matrigel Transmigration Analysis

Cells from each clone were suspended in Dulbecco's modified Eagle's medium or F12K medium containing 0.1% bovine serum albumin added to the upper chamber at 1×10^5 cells/insert. A conditioned medium obtained by incubating NIH 3T3 cells for 24 hours in serum-free Dulbecco's modified Eagle's medium in the presence of 50 μg/ml ascorbic acid were placed in the lower compartment of the invasion chambers as chemoattractants. After 24 hours of culture, the upper surfaces of the inserts were wiped with cotton swabs, and the inserts were stained with hematoxylin and eosin. Each experiment was performed twice with each sample in triplicate. The cells that migrate through the Matrigel and the filter pores

to the lower surface were counted under a light microscope with five random high-power fields per insert.

Tumor Growth and Spontaneous Metastasis Assay

SCID mice were subcutaneously implanted at the abdominal flank with 1×10^7 viable cells, suspended in 0.2 ml of Hanks' balanced salt solution. The animals were observed daily. Body weight, tumor size, and other special findings, including lymph-node enlargement, were recorded weekly. After 12 weeks or when the mice became moribund, they were sacrificed, and autopsies were performed. Serial sections of lung, brain, liver, kidneys, vertebra, and lymph nodes were performed. These tissues were formalin-fixed and paraffin-embedded. The sections were stained with hematoxylin and eosin and subject to histology examination. All studies were approved by the University of Pittsburgh Institutional Animal Care and Use Committee (IACUC).

Fluorescence in Situ *Hybridization*

Cells grown on chamber slides were fixed in 100% ethanol for 2 minutes, and air-dried. Fluorescence *in situ* hybridization was performed as follows: slides were placed in 2× standard saline citrate at 37°C for 30 minutes. Slides were then removed and dehydrated in 70% and 85% ethanol for 2 minutes each at room temperature, and air-dried. The probe was prepared by combining 7 μl of biotin-labeled genomic sequence containing myopodin (12 kb)/50% formamide with 1 μl of direct-labeled CEP4 Spectrum Orange (Vysis, Downers Grove, IL). The probe was denatured for 5 minutes at 75°C. Chamber slides were denatured in 70% formamide for 3 minutes, and dehydrated in 70%, 85%, and 100% ethanol for 2 minutes each at room temperature. The denatured probe was placed on the slide, coverslipped, sealed with rubber cement, placed in a humidified chamber, and hybridized overnight at 37°C in a humidified chamber. Posthybridization washes were performed by removing the coverslip, and placing the slide in 2× standard saline citrate/0.3% Nonidet P-40 at 72°C for 2 minutes. Slides were then placed in PBS at room temperature in the dark for 2 minutes. The biotin label was visualized by placing avidin-fluorescein isothiocyanate (FITC) (Zymed, San Francisco, CA) on the slide, coverslipping, and placing in a moist chamber in the dark at 37°C for 20 minutes. Slides were washed three times for 2 minutes each in fresh PBS. Slides were air-dried in the dark and counterstained with 4,6-diamidino-2-phenylindole. Analysis was performed using a Nikon Optiphot-2 and Quips Genetic Workstation equipped with Chroma Technology 83000 filter set with single band exitors for Texas Red/rhodamine, FITC, 4,6-diamidino-2-phenylindole (UV 360 nm). Only individual and well-delineated cells with two hybridization signals were scored. Overlapping cells were excluded from the analysis.

Immunohistochemistry Staining and Tissue Array Analysis

Formalin-fixed and paraffin-embedded human prostate tissues including prostate cancer (n = 78) and normal prostate samples (n = 28) from 106 individuals were arrayed onto slides in a format of quadruplicate representation for each sample. The ages of patients range from 15 to 79. Complete 3-year follow-up data are available for all 78 cases of prostate cancer patients. For immunostaining, 4-μm-thick sections of tissue array was cut and mounted on glass slides. The sections were heated at 60°C for 12 hours and deparaffinized in xylene and ethanol. Antigen retrieval was performed using 25 mmol/L sodium citrate buffer (pH 9.0) at 90°C for 15 minutes, followed by treatment of 3% H_2O_2 to block endogenous peroxidase. The slides were incubated at room temperature for 2 hours with anti-myopodin antibodies at 1:400 dilution. The sections were then incubated with horseradish peroxidase-conjugated anti-rabbit IgG for 30 minutes at room temperature. This was followed by incubating the section with 3,3′-diaminobenzidine solution (DAKO, Carpinteria, CA) to develop staining color. Hematoxylin was used for counterstaining. The specificity of immunostainings were verified by incubating the similar slides with preimmune sera.

Results

Hemizygosity and Expression of Myopodin in Prostate Cancer Cell Lines PC-3, DU145, and LNCaP

Myopodin was found preferentially deleted in advanced stage prostate cancer. To examine the allele status of myopodin in three metastatic prostate cancer cell lines (PC-3, DU145, and LNCaP), fluorescent *in situ* hybridization using genomic probes that span the entire myopodin region was performed on PC-3, DU145, and LNCaP cells. As shown in Figure 1A, signals of myopodin (FITC) and chromosome 4 centromere (Spectrum Orange) were tabulated on 50 cells for normal lymphocytes and for each of the prostate cancer cell lines. The signal ratios of myopodin to centromere were calculated as 1.05, 0.31, 0.29, and 0.45 for normal lymphocytes, PC-3, LNCaP, and DU145, respectively. These results clearly indicate hemizygous status of myopodin in these prostate cancer cell lines. To examine the myopodin expression of PC-3, DU145, and LNCaP, we performed reverse transcriptase (RT)-PCR (Figure 1B) and immunoblot analysis (Figure 1E) using anti-serum against myopodin C-terminus. A small amount of myopodin was detected by RT-PCR in PC-3 and DU145, but no myopodin was identified in LNCaP at either mRNA or protein level. Other mechanisms, such as methylation or down-regulation of a critical transcription factor or a small deletion or mutation in the mRNA start site, etc, might play a role in inhibiting myopodin expression besides hemizygosity.

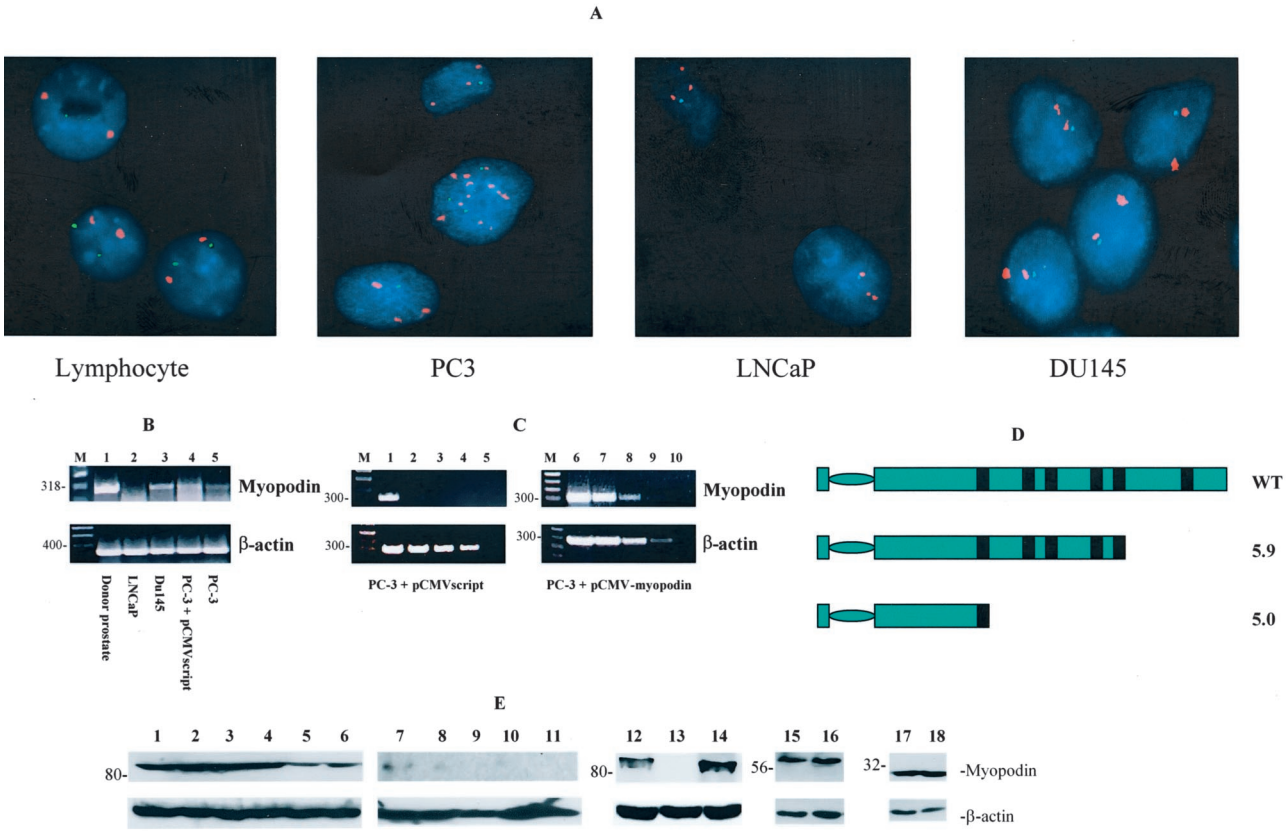

Figure 1. Hemizygosity and expression of myopodin in prostate cancer cell lines. **A:** Fluorescence *in situ* hybridization of myopodin genome sequence and chromosome 4 centromere in normal lymphocytes (**left 1**), PC-3 cells (**left 2**), LNCaP (**left 3**), and Du145 (**left 4**). Chromosome 4 centromere was labeled with spectrum orange and myopodin was labeled with FITC. **B:** RT-PCR of myopodin gene on mRNA extracted from normal donor prostate tissue (**lane 1**), LNCaP (**lane 2**), Du145 (**lane 3**), PC-3 cells transfected with control vector pCMV-script (**lane 4**), and PC-3 cells (**lane 5**). Primers specific to β-actin were used as controls. **C:** Semiquantitative RT-PCR of myopodin mRNA in PC-3 cells transformed with myopodin expression vector (clone I4, **lanes 6** to **10**) and with control vector (clone P2, **lanes 1** to **5**). The templates were subsequently diluted to 0 (**lanes 1** and **6**)-, 10 (**lanes 2** and **7**)-, 100 (**lanes 3** and **8**)-, 1000 (**lanes 4** and **9**)-, and 10,000 (**lanes 5** and **10**)-fold. Primers corresponding to β-actin were used as controls. **D:** Schema of wild-type myopodin and its mutant 5.9 and 5.0. **Black stripes** represent homologous sequence with synaptopodin. **E:** Immunoblotting of myopodin from different prostate cancer cell lines. Protein extracts from PC-3 cells transformed with pCMV-myopodin (**lanes 1** to **4** for clones I1, I2, I8, and I4, respectively), PC-3 cells transformed with pCMVscript (**lanes 7**-**9** for clone P1–3 respectively), and LNCaP cells transformed with pCMV-myopodin (**lanes 5** to **6** for clone LM9 and LM25, respectively), LNCaP cells transformed with pCMVscript (**lanes 10** and **11** for clone LP2 and LP6, respectively), primary normal prostate epithelial culture 5 (**lane 12**), prostate cancer 7270 (**lane 13**), normal prostate donor PD20 (**lane 14**), myopodin deletion mutant 5.9 (**lanes 15** and **16** for clones 10 and 8, respectively), and 5.0 (**lanes 17** and **18** for clones 12 and 3, respectively).

Overexpression of Myopodin in PC-3 and LNCaP Cells Using Eukaryotic Expression Vector pCMV-Myopodin Inhibits Growth and Suppresses Invasion

To investigate the potential tumor suppression effect of myopodin, we overexpressed myopodin in PC-3 and LNCaP cells by constructing myopodin cDNA into a constitutive eukaryotic expression vector (pCMV-script). Fifteen colonies were isolated from each of the pCMV-myopodin-transformed LNCaP and PC-3 cells and from the corresponding controls (pCMV-script). The myopodin expression levels were then examined in immunoblot using antiserum against myopodin. Fourteen of these clones were found to overexpress myopodin by 10- to 100-fold in protein levels over the vector-only transformed cells (Figure 1E). After expression of myopodin protein in transformed cells was confirmed (Figure 1C), two of these colonies were selected for cell proliferation assay. As shown in Figure 2, both LNCaP and PC-3 transformed with pCMV-myopodin increase the cell doubling time from an average of 3 days (PC-3) and 4 days (LNCaP) to >6 days and >9 days, respectively, suggesting myopodin suppressed the proliferation of these prostate cancer cells. To examine the effect of myopodin on the ability of tumor cells to form colony from a single cell, we performed colony formation assays on myopodin-transformed PC-3 and LNCaP cells. As demonstrated in Figure 3, the myopodin-transformed PC3 and LNCaP cells showed 2.5 ($P < 0.002$)- and 3.2 ($P < 0.0003$)-fold decrease, respectively, in colony numbers. These results suggest that myopodin inhibits tumor colony formation and cancer volume expansion.

To evaluate the role of myopodin in cancer invasion and metastasis, we examined the effect of myopodin on invasiveness of PC-3 and LNCaP through Matrigel transmigration and soft agar colony formation analysis. As shown in Table 1, the motile ability of myopodin-transformed clones was virtually identical to the control cell lines. However, myopodin significantly reduced the trans-

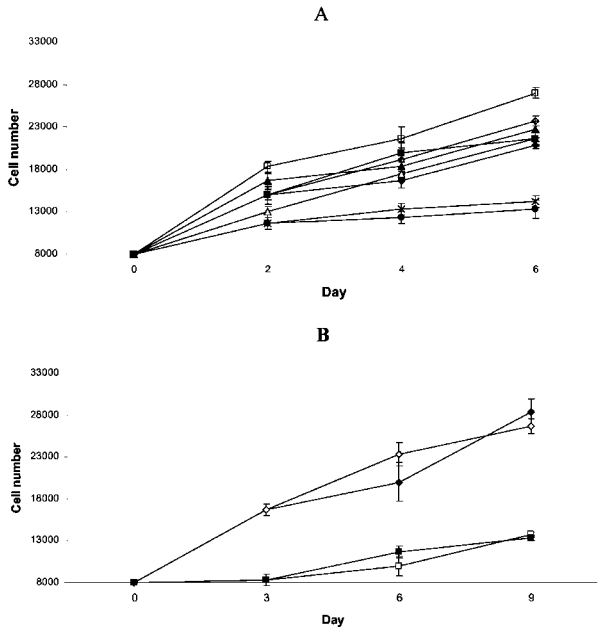

Figure 2. Myopodin expression suppresses proliferation of PC-3 and LNCaP cells. **A:** Two colonies of PC-3 cells transformed with myopodin expression vector (I4, ×; I8, ●) or control vector (P2, ◇; P3, ▲) or myopodin mutants deleted 179 amino acids (5.9 no. 10, □; 5.9 no. 8, ◆) or myopodin mutants deleted 470 amino acids at its C-terminus (5.0 no. 12, △; 5.0 no. 3, ■) were selected for proliferation analysis. Eight thousand cells were initially plated and cell numbers were counted at the indicated time. **B:** Two colonies of LNCaP cells transformed with myopodin expression vector (LM9, ■; LM25, □) and expression vector control (LP2, ◆; LP6, ◇). Similar experiments were performed as in **A**. Each **point** represents an average of triplicate experiments with a SE.

migration rate of both PC-3 and LNCaP cells in these *in vitro* invasion analyses by up to fivefold. This inhibition was reversed when the expression of myopodin was inhibited by a cocktail of myopodin anti-sense oligonucleotides. Colony formation in soft agar produced >90% inhibition of PC-3 colony formation in soft agar with myopodin transformation (Figure 4), indicating a significant inhibition of PC-3 cell growth in a three-dimensional space.

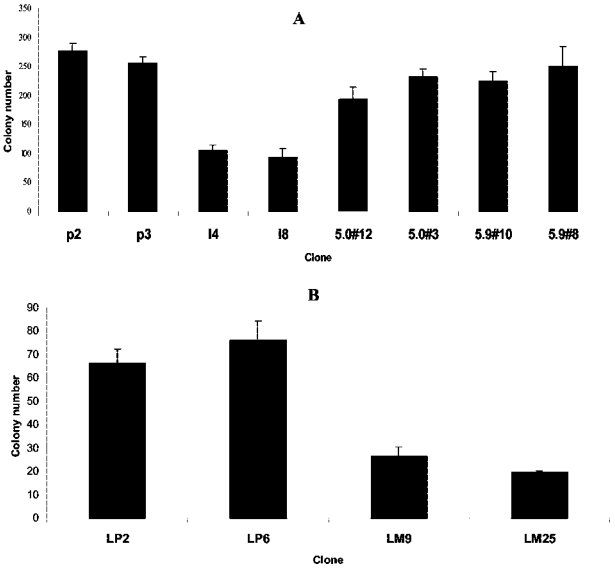

Figure 3. Myopodin expression suppresses colony formation of PC-3 and LNCaP cells. Triplates of 5000 cells of indicated lineages were plated on 35-mm diameter dishes. Colonies larger than 0.2 cm in diameter were tabulated at the 10th day of the culture. **A:** Cells derived from PC-3. **B:** Cells derived from LNCaP. Each column represents an average of triplicate experiments with a SE.

To investigate whether myopodin inhibits tumor growth and metastasis *in vivo*, PC-3 cells with (pCMV-myopodin clone I4 and I8) or without (pCMV clone P2 and P3) myopodin expression were transplanted into SCID mice subcutaneously. As shown in Table 2, the average size of the xenografted PC-3 cell tumors transformed with pCMVscript vector control is 5.28 cm^3 (4.86 and 5.71 cm^3 for P2 and P3 tumors, respectively), whereas the average size for pCMV-myopodin-transformed PC-3 cell tumors is 0.87 cm^3 (0.44 and 1.32 cm^3 for I4 and I8, respectively). This represents a sixfold reduction in tumor size. Using the Wilcoxon rank-sum test, tumors are significantly smaller in the myopodin group ($P < 0.001$). Five incidences of invasion or metastasis were observed in vector control group and none was found in myopodin one. Six mice from the vector control group became severely moribund and were euthanized within 6 weeks of tumor inoculation but none from myopodin. These results demonstrate that myopodin expression reduces metastasis and cancer mortality.

Tumor Suppression Activity of Myopodin Is Located at the C-Terminus

The function of myopodin in epithelial cells remains speculative. To investigate which domain of myopodin is crucial in inducing tumor growth and metastasis suppression, we constructed two deletion mutants that have the C-terminal region deleted. These deletion mutants would partially or mostly delete synaptopodin homologous sequences. The deletion mutants generate truncated myopodin mutants with molecular weights of 60 and 28 kd for mutants 5.9 and 5.0, respectively (Figure 1E). These mutants were constructed into pCMV-script expression vector and subsequently transfected and overexpressed in PC-3 cells. Both colony formation and cell proliferation analyses indicate that both types of deletions abrogate the myopodin tumor growth suppression activity. Similarly, both deletions reverse the myopodin effect on PC-3 cells in transmigration and soft agar colony formation assays. These results clearly indicate the important role of C-terminus region of myopodin in inducing tumor suppression.

Expression of Myopodin Is Inversely Correlated with the Progression of Human Prostate Cancer

To examine the involvement of myopodin in the progression of prostate cancer, the expression of myopodin in tissue samples was analyzed by immunostaining in 78 prostate cancers with various Gleason grades. We divided the prostate cancer samples into two groups based on the observed clinical aggressiveness, in which an aggressive tumor is defined by any of the following:

Table 1. Matrigel Transmigration Analyses of Myopodin-Transformed PC-3 and LNCaP Cells*

Cell ratios	Cells invading through Matrigel HPF†	Cells in control membrane HPF	Invasion/migration
PC-3 + pCMV			
Clone P1	28.2 ± 2.5	43.4 ± 5.1	0.65
Clone P2	20.6 ± 1.4	25.5 ± 2.3	0.82
Clone P3	18.4 ± 1.6	24.9 ± 2.9	0.74
PC-3 + pCMV-myopodin			
Clone I1	5.2 ± 1	37.5 ± 5.4	0.14
Clone I2	5.6 ± 1.3	29.4 ± 2.7	0.19
Clone I8	3.0 ± 0.9	27.2 ± 2.5	0.11
Clone I4	3.8 ± 2.2	29.2 ± 3.1	0.13
Clone I4 + anti-sense	25.5 ± 5.1	35.6 ± 3.8	0.71
Clone I4 + sense	5.2 ± 2.1	24.8 ± 4.2	0.21
PC-3 + pCMV-myopo5.9‡			
Clone 5.9 no. 8	30.6 ± 5.6	48.3 ± 6.3	0.63
Clone 5.9 no. 10	24.7 ± 6.1	40.6 ± 7.2	0.61
PC-3 + pCMV-myopo5.0§			
Clone 5.0 no. 3	28.3 ± 3.2	35.2 ± 5.9	0.80
Clone 5.0 no. 12	23.5 ± 4.4	32.6 ± 3.7	0.72
LNCaP + pCMV			
Clone LP2	34.1 ± 5.2	48.2 ± 6.3	0.70
Clone LP6	33.8 ± 7.1	66.3 ± 8.2	0.51
LNCaP + pCMV-myopodin			
Clone LM9	7.8 ± 1.2	68.4 ± 6.7	0.11
Clone LM25	3.4 ± 0.7	78.7 ± 9.2	0.04

*The pCMV-transformed PC-3 and LNCaP cells and their myopodin-transformed counterparts will be suspended in DMEM containing 0.1% bovine serum albumin and added to the upper chamber at 1×10^5 cells/insert. The inserts contained an 8-μm pore-size membrane with a thin layer of Matrigel basement membrane matrix. Controls were those containing basement membrane but no insert in the chamber.
†Mean of five experiments with standard errors. HPF-per high-power field.
‡Myopodin expression vector with partial deletion of synaptopodin homologous sequence.
§Myopodin expression vector with complete deletion of synaptopodin homologous sequence.

cancer invasion into adjacent organs or seminal vesicles, clinical relapse evidenced by an increase of prostate-specific antigen level after radical prostatectomy, or distant metastasis. Organ-confined tumors were defined by lacking the above features regardless of tumor differentiation. As shown in Figure 5A, myopodin was highly expressed in the epithelial cells of normal glands. The basal cells also show a good level of staining, whereas stromal fibroblasts have minimal expression of myopodin. Smooth muscle and skeletal muscle were also stained with myopodin antibodies. Endothelial cells have no detectable myopodin expression. Interestingly, myopodin was primarily located in the nuclei but had occasional distribution in the cytoplasm. The expression of myopodin was graded as strong (2 points), weak (1 point), or negative (0 points) for each sample. The overall score for each sample represents the average of scores for four locations of the same sample. Thus, the score range from 0 to 0.5 is considered negative, 0.5 to 1.5 is weakly positive, and 1.5 to 2.0 is strongly positive. The myopodin expression was detected in all cases of normal prostate tissues, including 67% strong positive whereas 30% of cancer cells with aggressive features have no expression of myopodin. Only 1 of 50 aggressive prostate cancer cases had strong myopodin expression (Figure 5B). The level of myopodin expression was statistically analyzed. Although down-regulation of myopodin is not associated with Gleason's grade ($P = 0.43$), organ-confined prostate cancer has significant weaker myopodin expression (Wilcoxon rank-sum test, $P < 0.03$) in comparison with benign prostate tissues. Strong association of myopodin expression suppression was associated with invasiveness of prostate cancer (Wilcoxon rank-sum test, $P < 0.003$). These results suggest an inverse correlation between the progression of prostate cancer and the expression of myopodin.

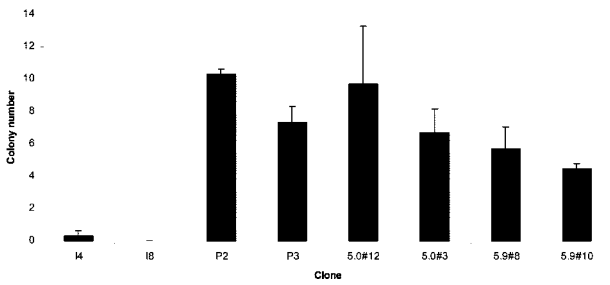

Figure 4. Myopodin expression suppresses colony formation of PC-3 cells in soft agar. Triplates of 5000 cells of indicated lineages were plated and grown on a plate containing 2% base agar and 0.43% top agar. Cells were incubated at 37°C for 21 days. Colonies were counted under dissecting microscope. Each column represents an average of triplicate experiments with a SE.

Discussion

Myopodin was identified almost simultaneously by two research groups using vastly different approaches.[3,4] Using the differential subtraction chain approach, we identified that myopodin was located within a minimum common deletion region of chromosome 4q25 among the prostate cancer cases. Southern blot and PCR survey studies indicated that myopodin was deleted in more than 50% of the aggressive prostate cancers. The protein encoded by myopodin shares significant homology with

Table 2. Myopodin Inhibits Growth and Metastasis of Xenografted PC-3 Cell Tumors in SCID Mice

Mouse	Tumor (PC-3 + pCMV)	M	PD	Mouse	Tumor (PC-3 + pCMV-myopodin)	M	PD
P2 tumor				I4 tumor			
1	3.15 cm^3 & 1.5 cm^3	None	No	1	0.72 cm^3	None	No
2	4.35 cm^3	Liver	Yes	2	0.35 cm^3	None	No
3	6.92 cm^3	None	No	3	0.43 cm^3	None	No
4	4.13 cm^3	None	No	4	0.12 cm^3	None	No
5	2.25 cm^3	None	No	5	0.08 cm^3	None	No
6	1.65 cm^3	Chest wall	No	6	0.01 cm^3	None	No
7	3.78 cm^3	None	No	7	0.67 cm^3	None	No
8	11.22 cm^3	Abdominal wall	No	8	0.36 cm^3	None	No
9	2.80 cm^3	None	No	9	0.67 cm^3	None	No
10	7.83 cm^3	None	Yes	10	0.94 cm^3	None	No
P3 tumor				I8 tumor			
1	8.56 cm^3	None	Yes	1	0.52 cm^3	None	No
2	7.83 cm^3	Vertebra	Yes	2	0.54 cm^3	None	No
3	3.85 cm^3	None	No	3	0.86 cm^3	None	No
4	4.64 cm^3	None	No	4	3.00 cm^3	None	No
5	3.31 cm^3	None	No	5	0.53 cm^3	None	No
6	4.29 cm^3	None	No	6	1.96 cm^3	None	No
7	5.58 cm^3	None	Yes	7	1.05 cm^3	None	No
8	6.34 cm^3	None	No	8	2.15 cm^3	None	No
9	7.51 cm^3	None	No	9	0.91 cm^3	None	No
10	5.23 cm	Chest wall	Yes	10	1.67 cm^3	None	No

M, metastasis; PD, premature death (died <6 weeks after tumor inoculation).

synaptopodin, whose expression is closely related to terminal differentiation of neurons and podocytes, and whose functions appear to form physiological contact with surrounding cells.[6,9] Further study indicated that deletion of myopodin, either partial or complete, was associated with high rates of metastasis and clinical relapse of prostate cancers. Hot spots of deletion were identified within the synaptopodin homologous region of myopodin. Absence of myopodin deletion, however, associated with low rate of invasion and clinical relapse regardless of the Gleason grades of the tumor. This study indicates that expression of myopodin is down-regulated in invasive prostate cancer. *In vitro* tumor suppression analysis indicates that expression of myopodin in invasive prostate cancer cell lines (PC3 and LNCaP) results in decreased invasiveness and suppression of cell proliferation. Consistent with these observations, the results of our animal experiments indicate that myopodin is capable of suppressing tumor growth, reducing invasion/metastasis and decreasing mortality in mice. Overall, myopodin appears to function as a tumor growth and dissemination suppressor.

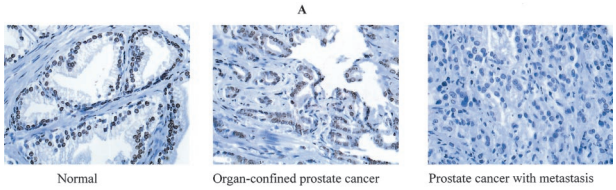

B

Myopodin Expression

	Strong positive	Weak positive	Negative
Benign prostate	19	9	0
Organ confined prostate cancer	7	21	0
Aggressive prostate cancer	1	34	15

Figure 5. Expression of myopodin protein is down-regulated in prostate cancer. Tissue array representing 78 prostate cancer and 28 normal prostate tissues were immunostained with antiserum against myopodin C-terminus. **A:** Representative images of immunostaining of myopodin in normal, organ-confined prostate cancer and prostate cancer with metastasis. **B:** Tabulation of myopodin expression in prostate tissue samples. The intensity of each staining was scored as negative (0), weak positive (1), strong positive (2.0). Overall score of a sample represents the average scores from four locations of the same specimen. Scores ranging from 1.5 to 2.0 are considered strong positive, 0.5 to 1.5 weak positive, 0.0 to 0.5 negative.

The molecular mechanism underlying the tumor suppression function of myopodin remains to be fully deciphered. Much of the clues about the function of myopodin might be implied through its homology with synaptopodin, which regulates cellular contacts. Besides containing sequence homologous to synaptopodin, myopodin also contains a proline-rich domain in the middle third of the protein. Another report suggested that myopodin interacted with β-actin and was involved in actin-bundling activity.[4] A recent report indicated that loss of myopodin expression in nucleus of urothelial cell carcinoma was predictive of poor clinical outcome. The expression of nuclear myopodin occurred at G_1/S phase of benign urothelial tissues but not from invasive cancer.[10] Our study indicates that deletion of myopodin in the region of C-terminus results in abolishment of tumor suppression function. Mutant 5.9, which contains a deletion of 197 amino acids at the C-terminus and eliminates only one small stretch of sequence (13 amino acids) homologous to synaptopodin, results in complete reversal of tumor suppression activity. This suggests that other motifs in the C-terminus region might also be important to tumor suppression activity. Although β-actin-bundling activity is difficult to quantify, the actin-binding activity appears to be impaired in mutant 5.9 in our initial explo-

rations (data not shown). This might be an epiphenomenon in our hands because this deletion encroaches into the minimal region necessary for actin binding by 62 amino acids as defined earlier.[4] It is of interest to note that myopodin is primarily distributed in the nucleus of normal epithelial cells. This is in contrast to the mature myocytes where myopodin is primarily distributed in Z-disk. It is only under stress that myopodin translocates to the nucleus to induce nuclear actin bundling in myocytes. Together, these findings suggest that myopodin might play different roles in myocytes and epithelial cells. It is plausible that nuclear actin binding and actin bundling are important to the tumor suppression activity of myopodin in epithelial cells, although definitive studies lie beyond the scope of the present communication.

An alternative argument about the mechanism of myopodin-induced tumor suppression is that overexpression of myopodin might be toxic to prostate cancer cells, and therefore, reduce the ability of myopodin-transformed cells to proliferate and to invade. To address this issue, FITC-conjugated annexin V was used to detect apoptosis or cell death after myopodin transformation. Fluorescence-activated cell sorting analyses were performed on several myopodin-transformed colonies. It appeared that myopodin did not significantly increase apoptosis of PC3 cells because similar proportions of cells stained with annexin V and propidium iodide were found in both the control and myopodin samples (data not shown). These initial findings are not consistent with the hypothesis that apoptosis is the major mechanism of myopodin-induced tumor suppression.

Pathogenesis of prostate cancer appears to require multiple stages and to be heterogeneous. Prospective follow-up studies performed in the 1980's and 1990's showed that some of the prostatic cancers developed from histologically defined epithelial precursor lesions referred to as high-grade dysplasia or high-grade prostatic intraepithelial neoplasia (PIN).[11,12] It is estimated that the risk for developing organ-confined prostate cancer is 20 to 60% for men with high-grade prostatic intraepithelial neoplasia.[11] The potential of organ-confined prostatic carcinoma to develop metastasis is also highly variable.[13] Large numbers of the prostate cancer cases are confined within the prostate for long period of time, and never develop clinical symptoms.[13] Only a small proportion of the cases develops metastasis and become life-threatening.[11,12] The process of developing metastasis and invasion is very complex, and is still poorly understood. Several underlying mechanisms are likely present for the development of such behavior. Because myopodin contains activity-suppressing tumor growth and invasion, it is possible that myopodin plays an important role in developing an invasive phenotype of prostate cancer. Consistent with this hypothesis, deletion or inactivation of expression of myopodin was most frequently identified in lesions characteristic of advanced stages of prostate cancer because it is lost in 30% of aggressive prostate cancer. Further investigation of the function of myopodin should shed some light on the complicated mechanisms of prostate cancer invasion and metastasis and provide clues for developing future therapeutic programs.

Acknowledgment

We thank Timothy Gavel for critical review and constructive comment on the manuscript.

References

1. Jemal A, Murray T, Samuels A, Ghafoor A, Ward E, Thun MJ: Cancer statistics, 2003. CA Cancer J Clin 2003, 53:5–26
2. Luo JH, Yu YP: Genetic factors underlying prostate cancer. Exp Rev Mol Med 2003, 5:1–26
3. Lin F, Yu YP, Woods J, Cieply K, Gooding B, Finkelstein P, Dhir R, Krill D, Becich MJ, Michalopoulos G, Finkelstein S, Luo JH: Myopodin, a synaptopodin homologue, is frequently deleted in invasive prostate cancers. Am J Pathol 2001, 159:1603–1612
4. Weins A, Schwarz K, Faul C, Barisoni L, Linke WA, Mundel P: Differentiation- and stress-dependent nuclear cytoplasmic redistribution of myopodin, a novel actin-bundling protein. J Cell Biol 2001, 155:393–404
5. Mundel P, Heid HW, Mundel TM, Kruger M, Reiser J, Kriz W: Synaptopodin: an actin-associated protein in telencephalic dendrites and renal podocytes. J Cell Biol 1997, 139:193–204
6. Mundel P, Reiser J, Zuniga Mejia Borja A, Pavenstadt H, Davidson GR, Kriz W, Zeller R: Rearrangements of the cytoskeleton and cell contacts induce process formation during differentiation of conditionally immortalized mouse podocyte cell lines. Exp Cell Res 1997, 236:248–258
7. Deller T, Mundel P, Frotscher M: Potential role of synaptopodin in spine motility by coupling actin to the spine apparatus. Hippocampus 2000, 10:569–581
8. Deller T, Korte M, Chabanis S, Drakew A, Schwegler H, Stefani GG, Zuniga A, Schwarz K, Bonhoeffer T, Zeller R, Frotscher M, Mundel P: Synaptopodin-deficient mice lack a spine apparatus and show deficits in synaptic plasticity. Proc Natl Acad Sci USA 2003, 100:10494–10499
9. Nagata M, Nakayama K, Terada Y, Hoshi S, Watanabe T: Cell cycle regulation and differentiation in the human podocyte lineage. Am J Pathol 1998, 153:1511–1520
10. Sanchez-Carbayo M, Schwarz K, Charytonowicz E, Cordon-Cardo C, Mundel P: Tumor suppressor role for myopodin in bladder cancer: loss of nuclear expression of myopodin is cell-cycle dependent and predicts clinical outcome. Oncogene 2003, 22:5298–5305
11. Bostwick DG: Progression of prostatic intraepithelial neoplasia to early invasive adenocarcinoma. Eur Urol 1996, 30:145–152
12. Scardino PT, Weaver R, Hudson MA: Early detection of prostate cancer. Hum Pathol 1992, 23:211–222
13. Raviv G, Janssen T, Zlotta AR, Descamps F, Verhest A, Schulman CC: Prostatic intraepithelial neoplasia: influence of clinical and pathological data on the detection of prostate cancer. J Urol 1996, 156: 1050–1055